Flux Position Estimation Method of IPMSM by Controlling Current Derivative at Zero Voltage Vector

Yuji Hosogaya*, Hisao Kubota*

Abstract – Various methods have been proposed to identify the flux position in an interior permanent magnet synchronous motor (IPMSM) without the use of mechanical sensors. To achieve this, a method that uses both the back electromotive force (EMF) and the saliency to identify the flux position in the IPMSM without the injection of high-frequency components at low speeds has been reported [16]. This method was then extended in order to drive the motor with no load to a light load [17][18]. We propose a combination of these methods with different proportional-integral (PI) controllers for controlling di_{dest}/dt and di_{qest}/dt. We also introduce compensation values F_L and F_H to reduce the position error when the estimation rule is being selected.

Keywords: IPMSM, Sensorless, Current derivative

1. Introduction

The permanent magnet synchronous motor (PMSM) is widely used because of its maintenance-free operation, high controllability, robustness against the environment, high efficiency, and high-power-factor operation. Appropriate control of the current vector is necessary for high-performance control. A high-performance control algorithm is often derived on the basis of a motor model [1]-[3]. The advantages of using interior PMSMs (IPMSMs) are that they have mechanically robust rotors owing to the magnets buried in the rotor core, and they utilize reluctance torque and field-weakening control.

However, IPMSMs use mechanical sensors such as rotary encoders to estimate the magnetic pole position information because the stator current of IPMSMs has to be controlled with pole position synchronization. However, the disadvantages to using a mechanical sensor are that it is expensive, unreliable, and occupies a lot of space. Therefore, various sensor-less control methods that estimate the magnetic pole position information using only current sensors were proposed in the early 1990s [4]-[7].

Some of these methods utilize electromotive force (EMF), which is proportional to the motor speed. These methods estimate the EMF with a disturbance observer, an estimation of current error, and a model reference adaptive system [8][9]. The pole position and rotor speed depends on the measurement and the direction of the EMF. Therefore, the use of these methods cannot be applied to IPMSM drives at low speeds or at a standstill because little or no EMF is generated in the low-speed region.

The other method used to estimate the pole position is by superimposing high-frequency components into the armature voltage commands of the motor [10]-[15]. This method is based on the magnetic saliency effect depending on the pole position, the current response by applying a pulse voltage, and the generated voltage high-frequency components current injection.

Although the aforementioned method enables the estimation of the pole position at the low-speed region and at a standstill, it generates a torque ripple and harmonic loss caused by the injection of high-frequency components. In addition, acoustic noise is also generated.

In contrast, a position estimation method in IPMSMs that uses both back EMF and saliency effects without an extra test signal such as the injection of high-frequency components was proposed [16]. Only standard current sensors—which are inherently used for the fundamental current control—are used to estimate the pole position at low speeds and at a standstill. However, this method cannot be used to estimate the pole position when the motor load is light.

Consequently, a pole position estimation method that enables estimation under no load to light load conditions was reported [17]. In order to estimate the pole position from no load to a rated load, a method that was a combination of those described in [16] and [17] was reported [18].

In this paper, we utilize two proportional-integral (PI) controllers for controlling the current derivatives: one for the light load condition and the other for the heavy load condition. We also introduce compensation values F_L and

* Graduate School of Science and Technology, Meiji University, Japan (kubota@isc.meiji.ac.jp)
Received 04 July 2011 ; Accepted 27 November 2011

F_H to reduce the position error that might occur while the estimation rule is being selected. This method requires only current sensors and does not result in high-frequency noise.

2. Method of identifying the flux position

,

The general voltage equation of the IPMSM is given below:

$$\begin{bmatrix} v_d \\ v_q \end{bmatrix} = \begin{bmatrix} R + pL_d & -\omega L_q \\ \omega L_d & R + pL_q \end{bmatrix} \begin{bmatrix} i_d \\ i_q \end{bmatrix} - \begin{bmatrix} 0 \\ \psi_f \omega \end{bmatrix} \tag{1}$$

i_d, i_q: Current in the d, q frame; R: Stator resistance; p: d/dt
L_d, L_q: Inductance in the d, q frame; Ψ_f: the back EMF constant; ω: rotating speed

When each output voltage is zero and the machine is running at low speed, the equation can be written as follows:

$$\begin{bmatrix} \dfrac{di_d}{dt} \\ \dfrac{di_q}{dt} \end{bmatrix} = -R \begin{bmatrix} \dfrac{1}{L_d} & 0 \\ 0 & \dfrac{1}{L_q} \end{bmatrix} \begin{bmatrix} i_d \\ i_q \end{bmatrix} - \begin{bmatrix} 0 \\ \dfrac{\psi_f \omega}{L_q} \end{bmatrix} \tag{2}$$

Let us suppose an estimated frame, dq_{est}, obtained by adding an angle θ_{err} to the dq frame (fig. 1). From (2), the relation between i_d-i_q and i_{dest}-i_{qest} is transformed into (3) and (4).

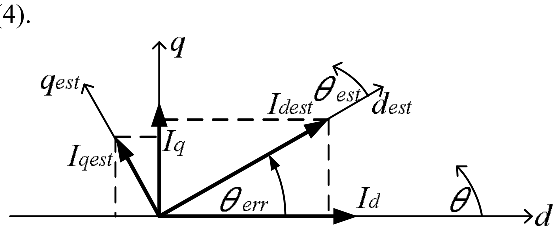

Fig. 1 Relation between dq frame and dq_{est} frame

$$\frac{di_{dest}}{dt} = \frac{R}{L_d L_q}\Big[\{(L_d - L_q)\cos^2\theta_{err} - L_d\} i_{dest} - \frac{1}{2}(L_d - L_q)\sin 2\theta_{err} \cdot i_{qest}\Big] - \frac{\psi_f \omega}{L_q}\sin\theta_{err} \tag{3}$$

$$\frac{di_{qest}}{dt} = -\frac{R}{L_d L_q}\Big[\frac{1}{2}(L_d - L_q)\sin 2\theta_{err} \cdot i_{dest} + \{(L_d - L_q)\cos^2\theta_{err} + L_q\}\, i_{qest}\Big] - \frac{\psi_f \omega}{L_q}\cos\theta_{err} \tag{4}$$

When the controller sets i_{dest} to zero, (3) can be simplified to (5). Thus, the position is estimated by controlling di_{dest}/dt to zero.

$$\frac{di_{dest}}{dt} = \frac{R}{2}\left(\frac{1}{L_d} - \frac{1}{L_q}\right) i_{qest} \cdot \sin 2\theta_{err} - \frac{\psi_f \omega}{L_q}\sin\theta_{err} \tag{5}$$

However, current deviation cannot be obtained accurately when i_{qest} is small. When i_{dest} is much greater than i_{qest}, (4) can be also be simplified to (6).

$$\frac{di_{qest}}{dt} = \frac{R}{2}\left(\frac{1}{L_d} - \frac{1}{L_q}\right) i_{dest} \cdot \sin 2\theta_{err} - \frac{\psi_f \omega}{L_q}\cos\theta_{err} \tag{6}$$

If di_{qest}/dt is controlled to zero, the component of back EMF becomes obstructed so as to make the position error tend to zero. However, this value is so small as to be negligible at low speeds or at a standstill. Thus, the flux position can be estimated by (6). Because the i_{qest} component is not included in (6), the load value is not considered.

We use two PI controllers for controlling the current derivatives, as shown in fig. 2.

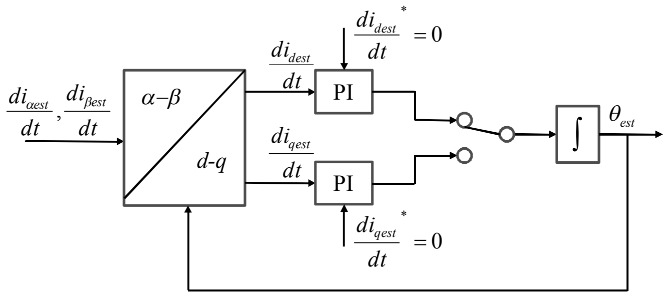

Fig. 2 Block diagram of flux position estimation

Calculation of the current differential is as follows. The three-phase currents are measured at any time instant within one cycle of the triangular carrier wave for pulse-width modulation (PWM) generation from m_1 to m_n, as shown in fig. 3. The longest pair of currents during a zero voltage vector, which is shown by V_0 or V_7 in fig. 3, is used to calculate current differential. Finally, the d or q-axis current differential is obtained by transforming the stationary frame to a rotational frame. Therefore, no additional sensors are required, such as voltage or current derivative sensors.

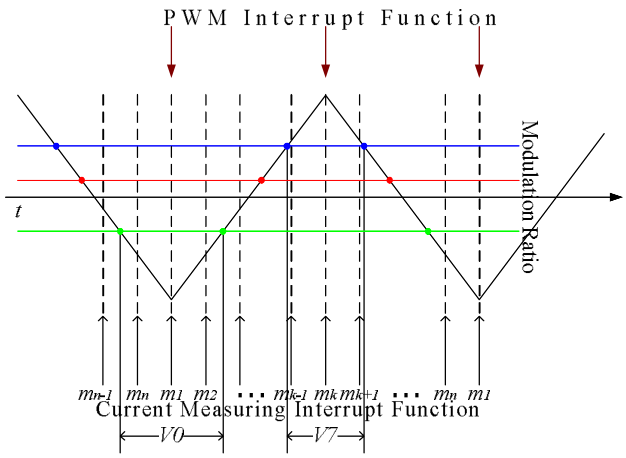

Fig. 3 Percent modulation and triangular wave current values

The current differential can be obtained easily since the time period of the zero vector voltage is relatively long in the low and zero speed regions of a PWM inverter. The pole position is estimated by applying the current differential to the PI controllers, as shown in fig. 2. In this method, acoustic noise is not generated as no extra test signal is injected, and the estimation algorithm is simple. In addition, this method is not influenced by parameter fluctuation.

3. Error compensation method at low load

As described above, (4) can be simplified to (6) on the condition that $i_{dest} >> i_{qest}$. However, when i_{qest} increases with an increase in the load, the simplification fails gradually, and it generates a steady error. Therefore, we propose the compensation method using v_d which is the voltage applied to the d axis. Despite i_d being set to a constant by the controller, v_d produces i_d and is also influenced by the pole position error. Thus, the compensation value can be obtained by comparing v_{dref} and v_{dest} (fig. 4). θ_{est} and v_{dref} can be represented as follows,

$$\theta_{est} = \theta'_{est} + \Delta\theta \tag{7}$$

$$v_{dref} = v_{dini} - \omega L_q \left(i_q - i_{qini}\right) \tag{8}$$

Both v_{dini} and i_{qini} are given by the experimental result, and are used to subtract the back EMF component.

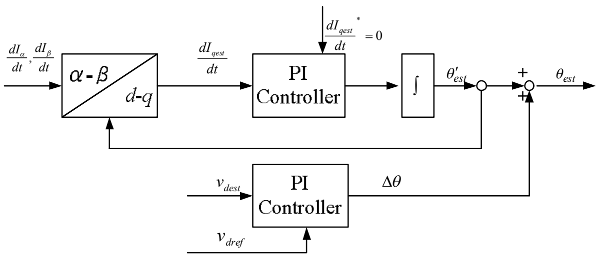

Fig. 4 Block diagram of error compensation at low load

4. Rule switching

According to section 2, we switch rules depending on the load applied to the motor. When the load is light, (6) is applied; when the load increases above a set value (5) is applied. However, since i_{dest} is not zero, (6) is applied and (5) is not applicable. In this condition, if θ_{err} is zero and i_{qest} is still much smaller than i_{dest}, which is set to a certain value with the light load, we can obtain (9) from (3).

$$\frac{di_{dest}}{dt} = \frac{R}{L_d L_q}\left(-L_q i_{dest}\right) = -\frac{R}{L_d} i_{dest} \tag{9}$$

Then, we define F_L as follows.

$$F_L = \frac{R}{L_d} \tag{10}$$

The following equation is obtained from (9) and (10).

$$\frac{di_{dest}}{dt} = -F_L i_{dest} \tag{11}$$

When (6) is applied, the estimation of the pole position for heavy load can be established by (11). After the speed feedback operation is switched to the estimation of the pole position for heavy load with (11), i_{dest} can be set to zero and (5) becomes applicable.

Similarly, when (5) is applied, (6) is not applicable, as i_{dest} is set to zero. In this condition, the following equation is obtained from (6),

$$\frac{di_{qest}}{dt} = -\frac{R}{L_d L_q} L_d i_{qest} = -\frac{R}{L_q} i_{qest} \tag{12}$$

Now, we define F_H as follows.

$$F_H = \frac{R}{L_q} \tag{13}$$

The following equation is obtained from (12) and (13),

$$\frac{di_{qest}}{dt} = -F_H i_{qest} \tag{14}$$

When (5) is applied, the estimation of the pole position for a light load is established by (14). After the estimation of the pole position for a light load is applied with (14), i_{dest} can be set to the certain value.

5. Experimental result of simulated machine

A simulation was carried out on a simulated machine using the same parameters as the actual machine (described in Table 1); the position sensor was also simulated in order to compare its results with those of the actual machine.

Table 1 Ratings and parameters of IPMSM actually used

1.5 kW, 170 V, 6.3 A, 6 poles, 87.5 Hz, 1750 min^{-1}, 8.0 Nm, R = 0.774 ohm, L_d = 8.90 mH, L_q = 11.96 mH, Ψ_f = 0.296 Wb

The carrier frequency was set to 4 kHz, and the currents are detected at 80 kHz to calculate the current derivatives.

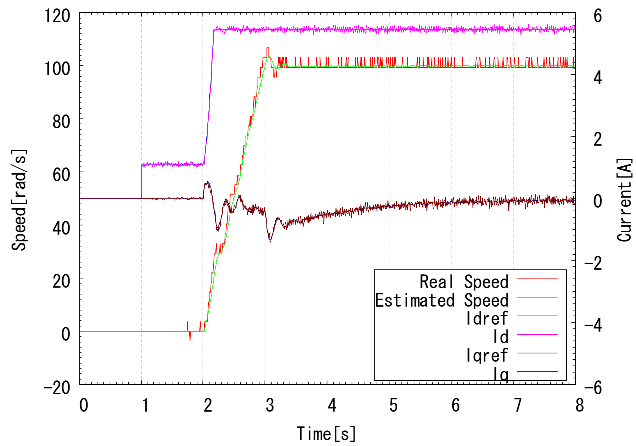

Fig. 5 Electrical speed and current at starting without load

We began the estimation of the pole position after the initial position of the rotor was obtained from the position sensor (fig. 5). Although the estimation can be calculated without the initial position, the oscillation of the rotor may generate a torque ripple at the start. The reference value of i_d relies on the speed until the speed reaches to 20 rad/s, then i_d is set to 50% of the rated current. Because the load torque is zero, i_q becomes negative.

To obtain the ramp input of the torque, the rated motoring load (fig. 6) and the rated regenerating load were applied to the machine while it was running at 100 rad/s (electrical speed) (fig. 7). The load was changed at 4 Nm/s. When i_d is controlled to zero, the estimation of the pole position for a heavy load is applied. As i_d is controlled to the certain value, the estimation of the pole position for the light load is applied. If i_q increases or decreases to the threshold value, the estimation of the pole position is automatically switched to either the light load rule or the heavy load rule. From the aforementioned data and figures, the switching method seems to work well.

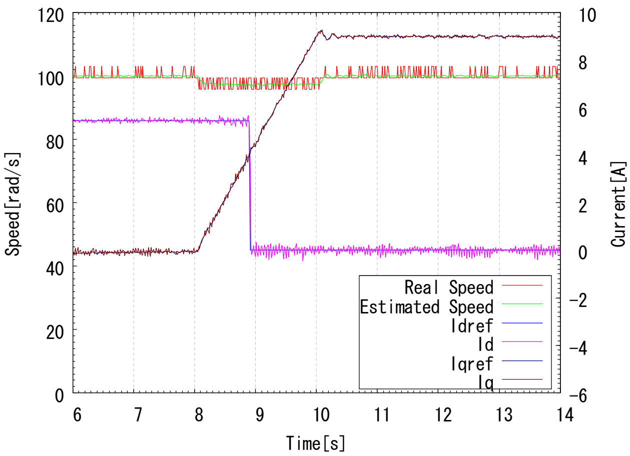

(a) No load to rated motoring load

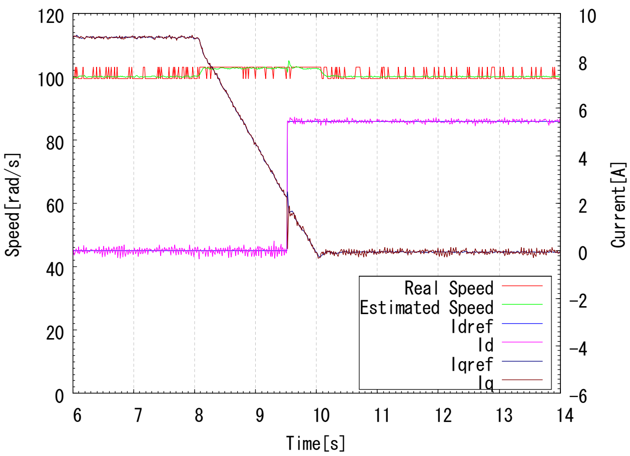

(b) Rated motoring load to no load

Fig. 6 Ramp input of torque (motoring load)

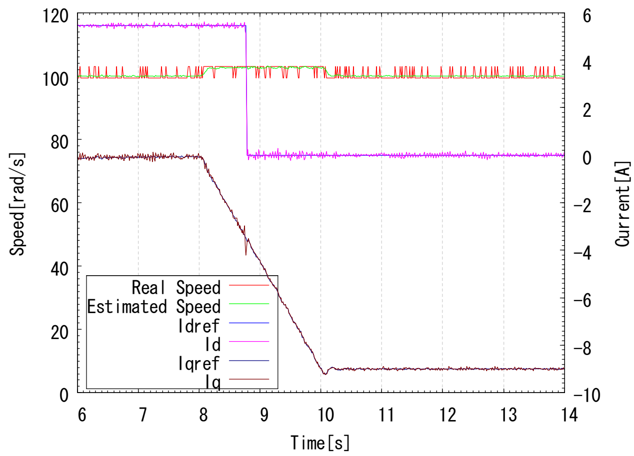

(a) Changed from no load to rated regenerating load

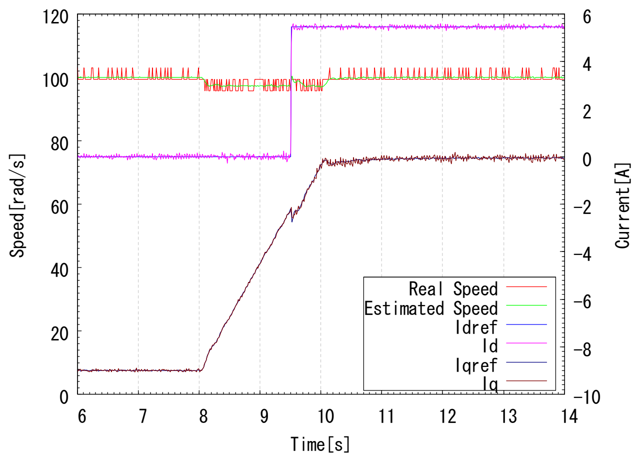

(b) Changed from rated regenerating load to no load

Fig. 7 Ramp input of torque (regenerating load)

The step input of the torque is also shown in fig. 8; this method was also found to work well with a rapid change in torque.

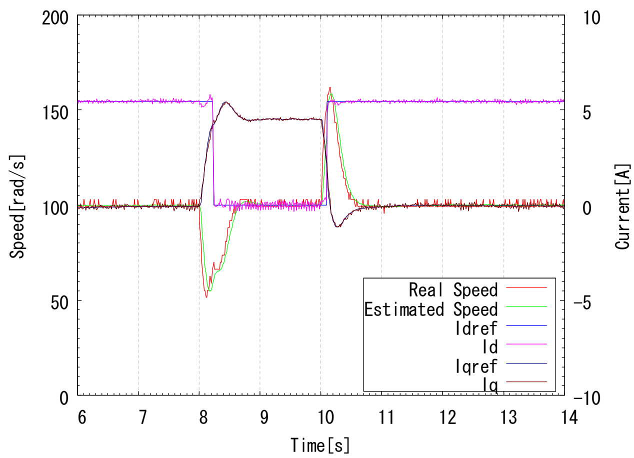

(a) No load to 50% of motoring load to no load

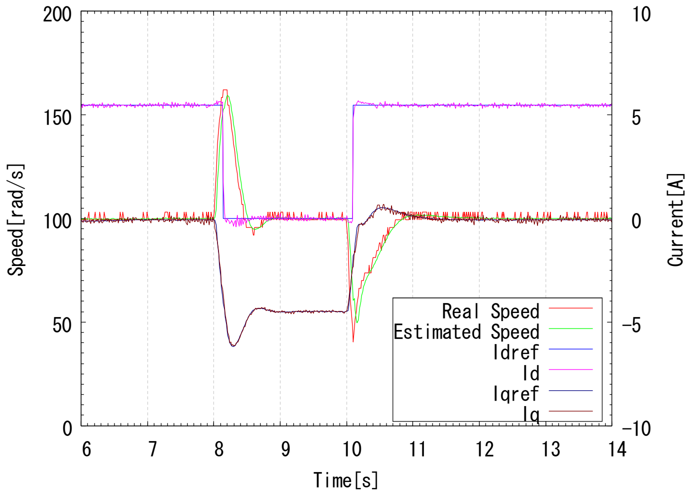

(b)No load to 50% regenerating load to no load

Fig. 8 Step input of torque

6. Experimental result of actual machine

Every experiment carried out with the simulated machine was also carried out with an actual machine. The carrier frequency was set to 4 kHz, and currents were detected at 80 kHz to calculate current derivatives.

After the initial position of the rotor was obtained from the position sensor, the pole position was estimated (fig. 9). To obtain the ramp input of the torque, as the machine was running at 100 rad/s, 80% of the motoring load was applied (fig. 10), and 80% of the regenerating load was applied (fig. 11). The load was changed at 4 Nm/s for these experiments.

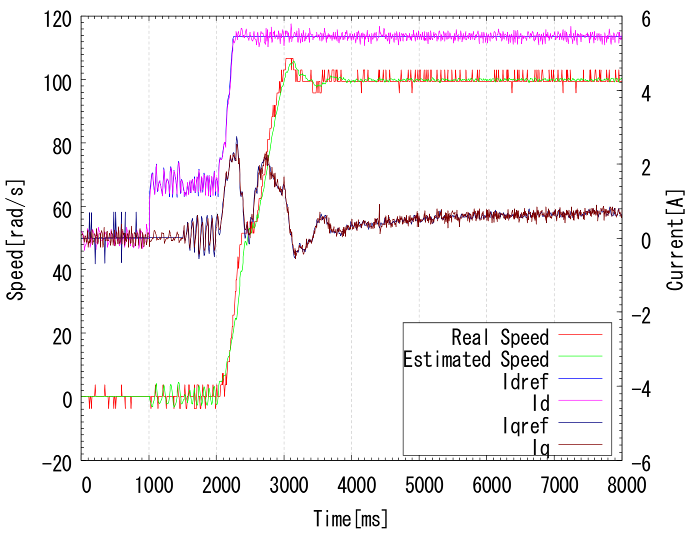

Fig. 9 Electrical speed and current at starting without load

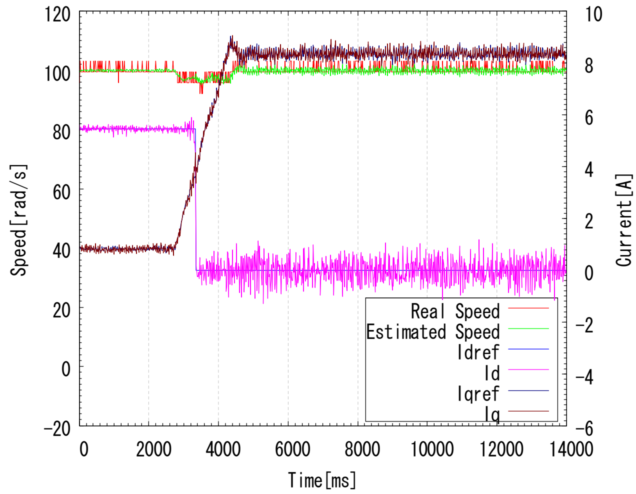

(a) No load to 80% of motoring load

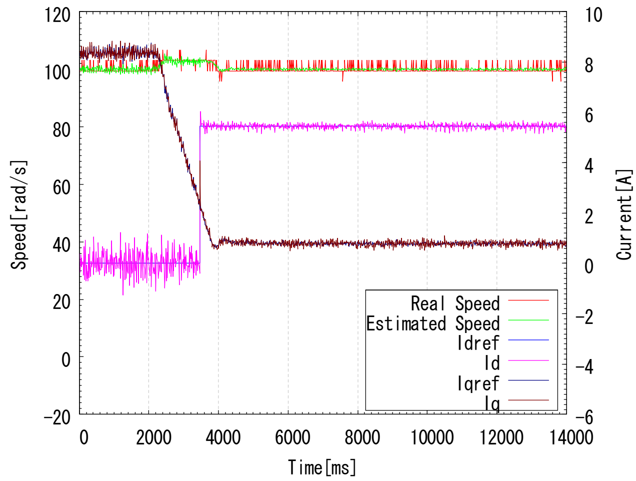

(b) 80% of the motoring load to no load

Fig. 10 Ramp input of torque (motoring load)

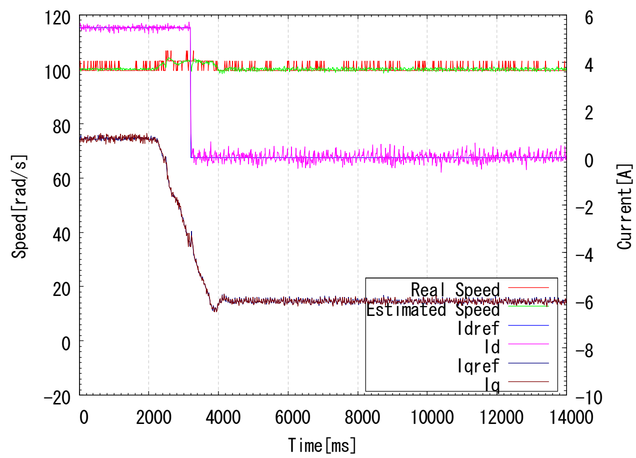

(a) Changed from no load to 80% of the regenerating load

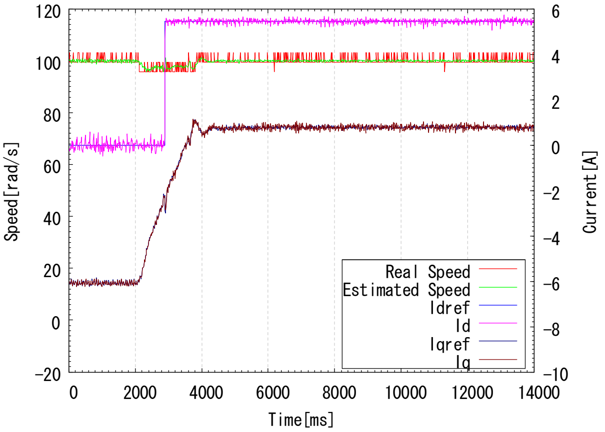

(b) Changed from 80% of the regenerating load to no load

Fig. 11 Ramp input of torque (regenerating load)

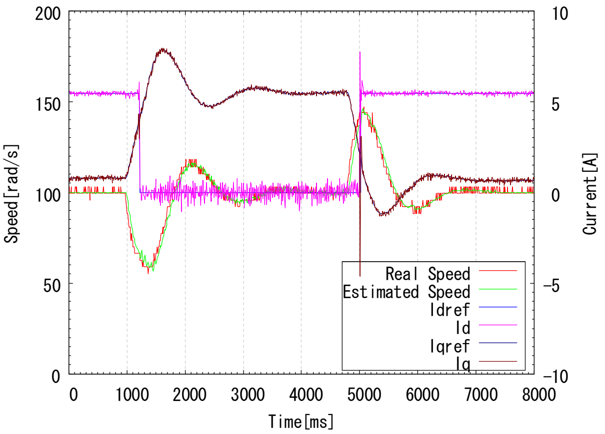

(a) No load to 50% of motoring load to no load

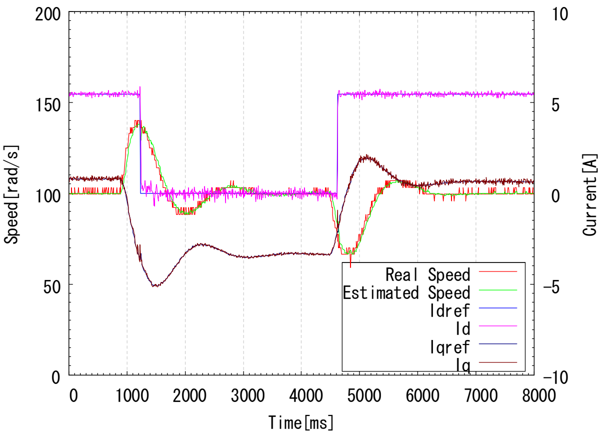

(b) No load to 50% of regenerating load to no load

Fig. 12 Step torque input

The step input of the torque is also shown in fig. 12; it is confirmed that the method also works well with the rapid change in torque.

7. Conclusion

In this paper, we proposed use of the position estimation method to find the flux position of an IPMSM using a switching method of a light load rule and a heavy load rule. The estimation rule is selected depending on the q-axis current. When the estimation rule is being selected, we utilize compensation values F_L and F_H to compensate for the error in the pole position. This method was validated by the experimental results of the simulated machine and the actual machine.

This position estimation method to find the flux position of IPMSMs uses both back EMF and saliency effects without an extra test signal such as an injection of high-frequency components. The advantages of this method are that there is no acoustic noise generated because no extra test signal is injected. The estimation algorithm is simple, and only uses standard current sensors, which are inherently used for fundamental current control to estimate the pole position. Thus, no additional sensors such as voltage or current derivative sensors are required.

References

[1] T. M. Jahns, G. B. Kliman, and T. W. Newmann, “Interior Permanent Magnet Synchronous Motors for Adjustable-Speed Drives,” *IEEE Trans. Ind. Appl.*, vol. IA-22, no. 4, pp. 738-747, Jul./Aug. 1986.

[2] S. Morimoto, Y. Takeda, and T. Hirasa, “Current Phase Control Methods for Permanent Magnet Synchronous Motors,” *IEEE Trans. Power Electron.*, vol. 5, no. 2, pp. 133-139, Apr. 1990.

[3] S. Morimoto, M. Sanada, and Y. Takeda, “Wide Speed Operation of Interior Permanent Magnet Synchronous Motors with High Performance Current Regulator,” *IEEE Trans. Ind. Appl.*, vol. 30, no. 4, pp. 920-926, Jul./Aug. 1994.

[4] Y. Iwaji, Y. Yamamoto, and H. Sugimoto, “Trends of Drive Circuit for Permanent Magnet Synchronous Motors,” in *Proceedings of the 2004 Japan Industry Applications Society Conference (JIASC2004),* no. 1-S152, pp. I(95) - I(106), 2004. (in Japanese)

[5] T. Fukumoto, N. Kitano, and K. Ohyama, “Technical Trends of AC Motor Drive Systems in Home Appliance,” in *Proceedings of the 2005 Annual Meeting Record IEE Japan*, vol. 4, no. 4-S17-5, pp. S17(18) - S17(23), 2005. (in Japanese)

[6] T. Noguchi, M. Ohshima, K. Kamiyama, T. Chin, H. Kubota, K. Shinohara, A. Chiba, S. Yamamoto, and H. Watanabe, “Technical Trends of AC Motor Drive Systems in Japan and Foreign Countries,” in *Proceedings of the 2005 Annual Meeting Record IEE Japan*, vol. 4, no. 4-S17-6, pp. S17(24) - S17(29), 2005. (in Japanese)

[7] J. Johnson and M. Shigyo, “Brushless DC Motor Control without Position and Speed Sensors,” *IEEE Trans. Industrial App.*, vol. 28, pp. 120-127, Jan./Feb. 1992.

[8] R. Tomioka, M. Nakano, G. Yang, and T. Chin, “Position and Speed Sensorless Control of Brush-Less DC Motor Based on

an Adaptive Observer," *Trans. IEE Japan D,* vol. 113-D, no. 5, pp. 579-586, May 1993. (in Japanese).
[9] S. Ichikawa, Z. Chen, S. Okuma, M. Tomita, and S. Doki, "Sensorless Controls of Salient-Pole Permanent Magnet Synchronous Motors Using Extended Electromotive Force Models," *Trans. IEE Japan D,* vol. 122-D, no. 12, pp. 1088-1096, Feb. 2002. (in Japanese).
[10] R. Masaki, S. Kaneko, Y. Sakurai, and M. Hombu, "Position Sensorless Control System of Brushless DC Motor Based on Voltage Injection Synchronized with PWM Carrier," in *Proceedings of the 2001 Japan Industry Applications Society Conference (JIASC2001),* vol. 1, no. 242, pp. 1247-1252, 2001. (in Japanese).
[11] T. Fukumoto, Y. Watanebe, H. Hamane, and Y. Hayashi, "A Method for Calculating AC Currents from Sampled DC Current Data in a Three-phase PWM Inverter," *Trans. IEE Japan D,* vol. 127-D, no. 2, pp. 181-188, Feb. 2007. (in Japanese).
[12] T. Kobayashi and H. Kubota, "Investigation of IPMSM's Position Estimation in Low Speed Region with DC Link Current Detection," in *Proceedings of the 22nd Annual IEEE Applied Power Electronics Conference and Exposition (APEC2007)*, vol. 2, no. D8.4, pp. 1411-1416, 2007.
[13] J. I. Ha, K. Ide, T. Sawa, and S. K. Sul, "Sensorless Rotor Position Estimation of an Interior Permanent-Magnet Motor From Initial States," *IEEE Trans. Ind. Appl.*, vol. 39, no. 3, pp. 761-767, May/Jun. 2003.
[14] M. J. Corley and R. D. Lorenz, "Rotor Position and Velocity Estimation for a Salient-Pole Permanent Magnet Synchronous Machine at Standstill and High Speeds," *IEEE Trans. Ind. Appl.*, vol. 34, no. 4, pp. 784-789, Jul./Aug. 1998.
[15] F. Briz, M. W. Degner, P. García, and R. D. Lorenz, "Comparison of Saliency-Based Sensorless Control Techniques for AC Machines," *IEEE Trans. Ind. Appl.*, vol. 40, no. 4, pp. 1107-1115, Jul./Aug. 2004.
[16] R. Raute, C. Caruana, J. Cilia, C. S. Staines, M. Sumner, "A Zero Speed Operation Sensorless PMSM Drive Without Additional Test Signal Injection," *The European Power Electronics 2007 (EPE 2007)*, 2007.
[17] Y. Shibano and H. Kubota, "Consideration about Pole Position Estimation Method of IPMSM at Low Speed without High Frequency Components Injection," in *Proceedings of the 2008 Annual meeting Record IEE Japan*, vol. 4, pp. 152-153, 2008. (in Japanese).
[18] Y. Shibano and H. Kubota, "Pole Position Estimation Method of IPMSM at Low Speed without High Frequency Components Injection," Applied Power Electronics Conference and Exposition, 2009 (APEC 2009).

Yuji Hosogaya received his Master of Engineering degree from Meiji university. His research interests are electric machines and motor driving.

Hisao Kubota received his B.E., M.E., and Ph.D. degrees in electrical engineering from Meiji University, Japan, in 1982, 1984, and 1989, respectively. Since 1984, he has been a member of the faculty at Meiji University, where he is currently a professor. His research interests focus on motor drives.
Dr. Kubota is a member of the Institute of Electrical Engineers of Japan. He is also a member of the IEEE Industry Applications, Industrial Electronics, and Power Electronics Societies.